J Mater Sci (2010) 45:1078–1085
DOI 10.1007/s10853-009-4046-y

Effect of sequence of nanoclay addition in TPU/PP blends: thermomechanical properties

M. Kannan · S. S. Bhagawan · Tomlal Jose · Sabu Thomas · Kuruvilla Joseph

Received: 6 July 2009 / Accepted: 17 November 2009 / Published online: 5 December 2009

Abstract Nanoclay filled thermoplastic polyurethane (TPU)/polypropylene (PP) blends compatibilized with maleic anhydride grafted polypropylene (MA-g-PP) have been studied with emphasis on sequence of nanoclay addition. In sequence I [TPU(nano)/PP/MA-g-PP], nanoclay was first added to TPU and this nano composite was blended with PP, using MA-g-PP as compatibilizer. In the case of sequence II [TPU/PP(nano)/MA-g-PP], nanoclay was added first to PP and blended with TPU, using MA-g-PP as compatibilizer. These blend systems were evaluated by DSC, FTIR, DMA, SEM, XRD and tensile properties. The results indicated that sequence I imparted greater compatibility to the polymers and better nanoclay dispersion than sequence II. Overall the TPU(nano)/PP/MA-g-PP blend system shows better dispersion than TPU/PP(nano)/MA-g-PP.

M. Kannan · S. S. Bhagawan
Department of Polymer Engineering, Amrita Vishwa Vidyapeetham, Coimbatore 641105, India
e-mail: m_kannan@cb.amrita.edu

T. Jose
Department of Chemistry, SB College, Changanachery 686101, Kerala, India

S. Thomas
School of Chemical Sciences, Mahatma Gandhi University, Kottayam 686560, India

K. Joseph (✉)
Department of Chemistry, Indian Institute of Space Science and Technology, Thiruvananthapuram 695022, Kerala, India
e-mail: kjoseph.iist@gmail.com

Introduction

Polyurethane is any polymer consisting of a chain of organic units joined by urethane links. Polyurethane polymers are formed by reacting a monomer containing at least two isocyanate functional groups with another monomer containing at least two alcohol groups in the presence of a catalyst. A urethane linkage is produced by reacting an isocyanate group (–N=C=O) with a hydroxyl (alcohol) group (–OH). PUs are composed of short, alternating polydisperse blocks of soft and hard segments (Fig. 1). The soft segment is typically a low glass transition temperature (T_g) polyether-, polyester- or polyalkyl diol. The hard segment is usually a high glass transition temperature, possibly semicrystalline, aromatic diisocyanate, linked with a low molecular weight chain extender. Thermoplastic polyurethanes are synthesized using a controlled molar ratio of isocyanate groups and chain extender, reducing the availability of free isocyanate groups for crosslinking. For optimal mechanical strength, this ratio is 1.0:1.1. In order to prevent crosslink formation, synthesis may be performed at temperatures below 80 °C to inhibit allophanate and biuret formation [1–3]. Polypropylene is a linear hydrocarbon polymer containing little or no unsaturation. The presence of a methyl group attached to alternate carbon atoms on the chain backbone can alter the properties of the polymer in a number of ways. The most significant influence of the methyl group is that it can lead to products of different tacticity, ranging from completely isotactic and syndiotactic structures to atactic molecules.

Cloisite® 10A (C10A) is a natural montmorillonite modified with quaternary ammonium salt. The organoclay used in this study (Cloisite 10A) was obtained from Southern Clay Products, USA. It is used to provide reinforcement and to modify various properties of polymers

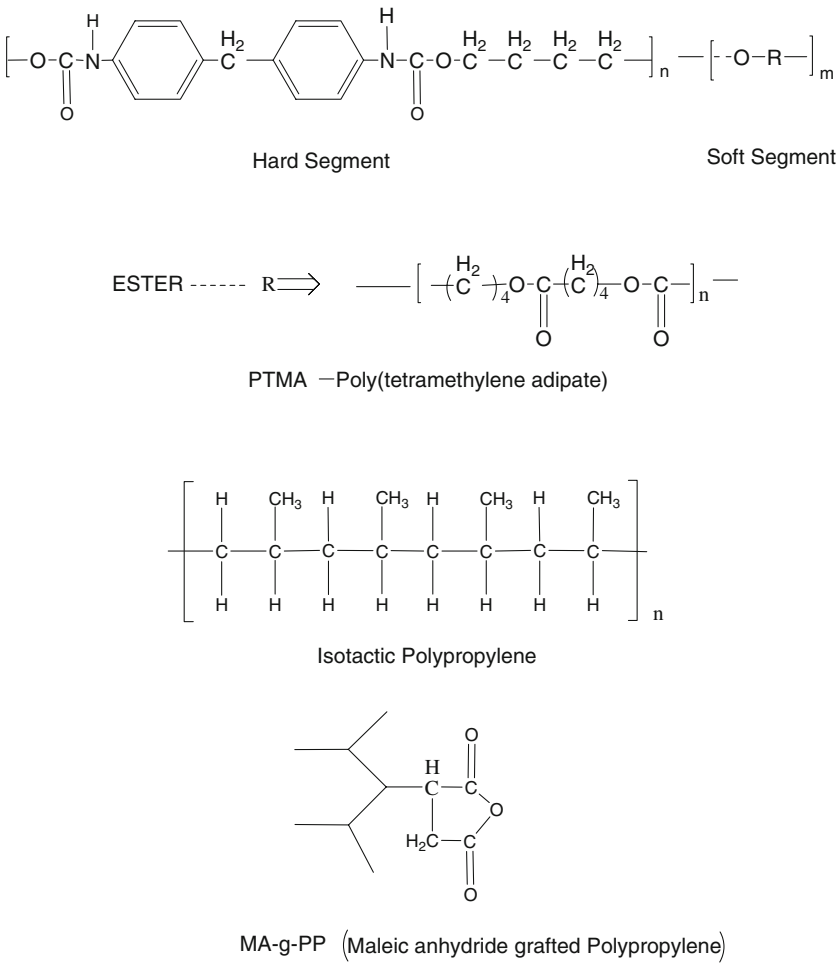

Fig. 1 Chemical structure of TPU, PP and MA-g-PP

like heat deflection temperature, coefficient of thermal expansion, flame retardancy and barrier performance [4, 5]. The organoclays are classified in different grades depending on the type and the amount of the organic cations. Functional groups in the cations are responsible for the hydrophobicity of the clay. Alkyl groups in organic cations make montmorillonite hydrophobic. On the other hand, polar groups like –OH result in hydrophilicity. Thermoplastic polyurethane and polypropylene form a highly incompatible blend due to their large differences in polarity and high interfacial tensions. However, TPU/PP blends have been prepared with an aim to reduce costs and improve the processability of polyurethane. The mechanical, thermal and chemical properties of polyurethane are improved by blending it with the polyolefin. Polyurethane, in turn, increases the impact strength, adhesion, printability and paintability characteristics of polypropylene.

Potschke et al. [6, 7], have studied the surface tension and interfacial tension of different PU and PP polymers. The reported experimental values indicated that low interfacial tension between polyether based TPU soft segment and PP results in better dispersion. Potschke et al. [8–10], have also carried out PP/TPU blend study without compatibilizers. They reported that, at similar viscosity ratios (μ_d/μ_m), blends with polyether based TPU produced a finer morphology than blends with polyester based TPU, due to low interfacial tension between their polyether based TPU soft segments and PP.

Lu et al. [11–13] have studied TPU/PP based blends in the ratio of 70/30 with compatibilizers like maleic anhydride-g-PP and primary/secondary amine-g-PP. Song et al. [14] investigated the phase morphology of nanoclay–polyurethane nanocomposite by small angle X-ray scattering (SAXS) and atomic force microscopy (AFM). It was observed that with increase in clay content, the surface energy of the polyurethane hard segments decreased from 45 dyne-cm/cm to 32 dyne-cm/cm for 3 wt% nanoclay loading. This result suggested that organic modification of nanoclay had a surface activation function to some extent. Compatibilization can be further improved by introducing functionalised PP (MA-g-PP) in the nanoclay containing blends [15–17].

The aim of the research described in this paper was to develop nanoclay filled TPU/PP blends with compatibilizer

to get overall best performance, using different nanoclay adding sequences in the blend system. In sequence I, nanoclay was first added to TPU and this nanocomposite was blended with PP, using MA-g-PP as compatibilizer. In the case of sequence II, nanoclay was added first to PP and blended with TPU, using MA-g-PP as compatibilizer.

Experimental

Materials

Ester-TPU (385 S) was supplied by Bayer (TPU) India Ltd., Chennai. The MFI value of 385 S is 10 g/10 min (190 °C/2.16 kg) with hardness value of Shore A 85. PP (MA 1100) was supplied by Reliance Industries Ltd., Jamnagar, India. The MFI value of PP (MA 1100) is 11 g/10 min (230 °C/2.16 kg). MA-g-PP compatibilizer was purchased from Pluss Polymers, New Delhi. The compatibilizer is a maleic anhydride functionalized polypropylene (MA-g-PP), containing 1 wt% of maleic anhydride. The MFI value of MA-g-PP compatibilizer is 12 g/10 min. (190 °C/2.16 kg).The organoclay used in this study (Cloisite 10A) was obtained from Southern Clay Products, USA. It is a Na^+ montmorillonite, chemically modified with dimethyl benzyl hydrogenated tallow quaternary ammonium ions (N^+ 2MBHT), where N^+ denotes quaternary ammonium ions, HT denotes hydrogenated tallow. HT is made of approximately 65% $C_{18}H_{37}$, 30% $C_{16}H_{33}$, and 5% $C_{14}H_{29}$. Cation exchange capacity is 125 meq/100 g clay.

Sequence I: TPU/C10A nanocomposites were prepared and subsequently blended with PP using MA-g-PP as compatibilizer. 3 wt% of the nanoclay was used. The ester–TPU pellets were dried at 100 °C for 4 h. The nanoclay was dried at 100 °C for 12 h in a vacuum oven. The dried pellets were fed into a co-rotating twin screw extruder and the temperature of the die zone was maintained at 190 °C. The extrudate was received as strands, which were cut into small granules for melt blending with PP. The granules of nanocomposites, along with pellets of PP and MA-g-PP were pre-dried at 100 °C for 4 h in a vacuum oven. Blending was done in the same co-rotating twin screw extruder with a die zone temperature of 190 °C and the extrudate was again obtained in the form of strands. Neat TPU/PP blends were prepared in the ratio of 70/30.

Sequence II: Nanoclay was added to PP by similar extruder melt blending and subsequently melt blended with TPU using MA-g-PP as compatibilizer (Table 1).

Testing and characterization

The change in gallery spacing of silicate layers in the blend nanocomposites was determined on an X-ray diffractometer (Bruker AXS D-8 Advance) using Cu ($\lambda = 1.54$ Å) as the radiation source. The samples were scanned at a rate of 3°/min (the increment step was 0.01° and the step time was 0.2 s) at room temperature for 2-theta values from 1° to 50°. The d-spacings were calculated using Bragg's equation ($n\lambda = 2d \sin \theta$).

The thermal properties of the blend nanocomposites were measured by a differential scanning calorimeter (Mettler Toledo, DSC 822e). Sample weight of 3–5 mg was scanned in nitrogen atmosphere at a heating rate of 10 K/min. Thermograms were taken by heating the samples in the temperature range from −100 °C to 300 °C.

The strands obtained after blending were cut into small granules for injection moulding. The prepared blend nanocomposites were moulded in an injection moulding machine (Ferromatik Milacron) to produce specimens for DMA test and tensile test. Dynamic mechanical measurements were performed for the prepared blend nanocomposites (60 mm × 13 mm × 3.5 mm) using a NETZSCH DMA 242 instrument provided with a dual cantilever. Analysis was done in the temperature range from −100 °C to 200 °C at a frequency of 10 Hz and a heating rate of 5 K/min. Tensile tests were carried out as per ASTM D 638 on a universal testing machine (International Equipments, Mumbai) at a crosshead speed of 200 mm/min. A maximum of 400% elongation was allowed and the stress required for 20, 100 and 200% elongation were recorded.

FTIR spectroscopy was performed for the prepared nanocomposites and blend nanocomposites in the ATR mode for convenience of measurement. A Thermo Nicolet (Avatar 370) spectrometer was used. Measurements were

Table 1 Compositions of ester–TPU based blend nanocomposites

Material	TPU (wt%)	TPU(C10A) (wt%)	PP (wt%)	PP(C10A) (wt%)	MA-g-PP (wt%)
TPU/PP	70	0	30	0	0
TPU/PP/MA-g-PP	70	0	25	0	5
TPU(C10A)/PP/MA-g-PP	0	70	25	0	5
TPU/PP(C10A)/MA-g-PP	70	0	0	25	5

Ester–TPU(C10A)—3 wt% nanoclay melt blended with TPU

PP(C10A)—8.4 wt% nanoclay melt blended with PP

done in the spectral range 4000–400 cm^{-1} at a resolution of 0.9 cm^{-1}. The injection moulded sample was immersed in xylene at 105 °C for 4 h to remove the PP portion in the TPU/PP blend. Morphological studies were performed on the solvent etched and gold sputtered samples using a JEOL (JSM-5800) Scanning Electron Microscope.

Results and discussion

XRD

X-ray diffraction (XRD) is extremely useful to study the structure and morphology of polymer nanocomposites [18–21]. As the layer spacing increases due to intercalation of polymer chains between the layers, the process can be monitored by X-ray diffraction. The diffraction characteristics of compatibilized TPU(C10A)/PP blends are shown in Fig. 2. In TPU/PP(C10A)/MA, a peak appears at $2\theta \sim 4.8°$ with reduced intensity as compared to neat nanoclay. This is an indication that the non-polar PP chains have been incorporated in the gallery space because of their affinity for the nanoclay. The peak is much weakened in ester–TPU(C10A)/PP/MA indicating some dispersion, it appears that the compatibilizer MA-g-PP aids the dispersion of nanoclay in the blend. XRD results are often reported to be misleading in terms of clay dispersion [16]. Therefore, only with the XRD analysis of these nanocomposites blends, it cannot be concluded that these nanocomposites show the intercalated or the exfoliated clay structures. In this regard, SEM images were taken and the results showed similar trend as XRD results. In the section on SEM analysis, effect of nanoclay dispersion is discussed with blend morphology of these blends.

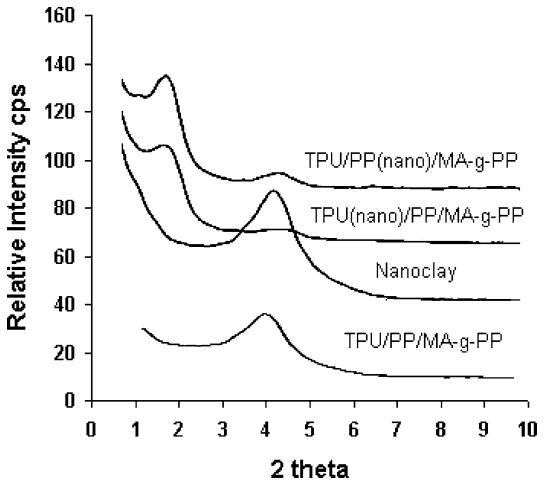

Fig. 2 XRD analysis

Differential scanning calorimetry

Differential scanning calorimetry (DSC) measures the amount of heat energy absorbed or released when the material is heated, cooled or maintained at a constant temperature. For polymeric materials, which undergo important property changes near thermal transitions, DSC is a very useful technique to study the glass transition temperature and melting behaviour [22–24]. The DSC thermograms of the TPU(C10A)/PP/MA blends are shown in Fig. 3. A summary of the observed thermal transitions is given in Table 2. In the case of both nanocomposites and blends, the TPU/PP(C10A)//MA materials showed a lower glass transition temperature of TPU(C10A)/PP/MA material. Compatibilization with MA-g-PP the T_g shift is more for TPU(C10A)/PP/MA blend nanocomposites, indicating better compatibility. The results showed that the TPU(C10A)/PP/MA blends were better compatibilized (T_g shifts from −57.5 to −47.5 °C) as compared to TPU/PP(C10A)/MA (T_g shifts from −57.5 to −50.3 °C). The difference between the melting point of PP (168 °C) and melting range of TPU (170–190 °C) is very narrow so the shift of T_m in the two blends was very small. This very small shift also may be influenced by factors like blend ratio and heating rate.

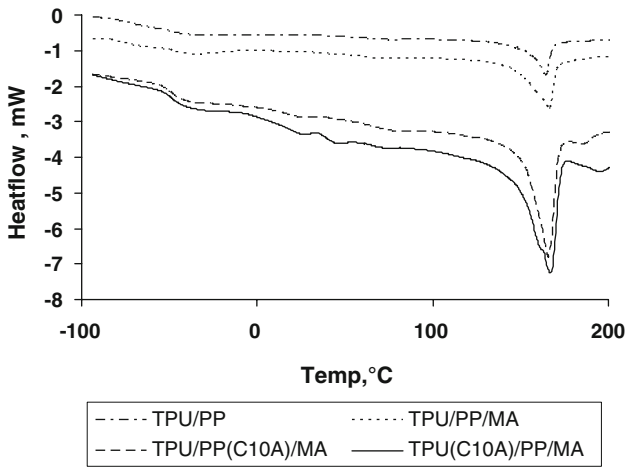

Fig. 3 DSC thermogram

Table 2 Thermal transitions from DSC for ester–TPU based blends

Material	T_g (°C)	T_m (°C)
TPU/PP	−60.2	167.9
TPU/PP/MA-g-PP	−57.5	168.0
TPU/PP(C10A)/MA-g-PP	−50.3	167.7
TPU(C10A)/PP/MA-g-PP	−47.5	167.7

Dynamic mechanical analysis

The variation of mechanical properties like storage and loss moduli can be studied as a function of temperature or frequency under a variety of deformation modes [25–29]. The ratio of the loss modulus (energy lost as viscous dissipation) and storage modulus (elastic energy stored during deformation) is known as tan δ and is indicative of the damping characteristics of the material. The dynamic mechanical parameters (storage modulus and loss modulus) for the various blend nanocomposites are plotted as a function of temperature, at a constant frequency of 10 Hz (Figs. 4, 5). The storage moduli for various selected temperatures are shown in Table 3.

The storage modulus at 20 °C of the TPU/PP blend, without nanoclay and compatibilized with the same wt% of MA-g-PP prepared under identical conditions, was 1.68 GPa. Thus, a 3 wt% C10A reinforcement increased the storage modulus of the blend by ~60% (2.64 GPa). At room temperature, the storage modulus value of the TPU(C10A)/PP/MA-g-PP blend nanocomposite was larger than that of the TPU/PP(C10A)/MA-g-PP blend nanocomposite. It is possible that well-dispersed clay platelets resulted in an increase in the storage modulus.

The dissipation factor (tan δ) of the materials are presented as a function of temperature in Fig. 4. The tan δ peak is associated with the soft segment glass transition temperature and the peak positions are given in Table 4. The temperature corresponding to the tan δ peak increases in the order TPU/PP < TPU/PP/MA-g-PP < TPU/PP(C10A)/MA-g-PP < TPU(C10A)/PP/MA-g-PP. This is attributed to the increasing order of compatibility for the blends. The same trend was observed in the plot of loss modulus versus temperature for the blends, thereby confirming the higher miscibility in compatibilized TPU(C10A)/PP/MA blends. The same order was observed in DSC experiment also. The T_g may have different numerical values but it follows the

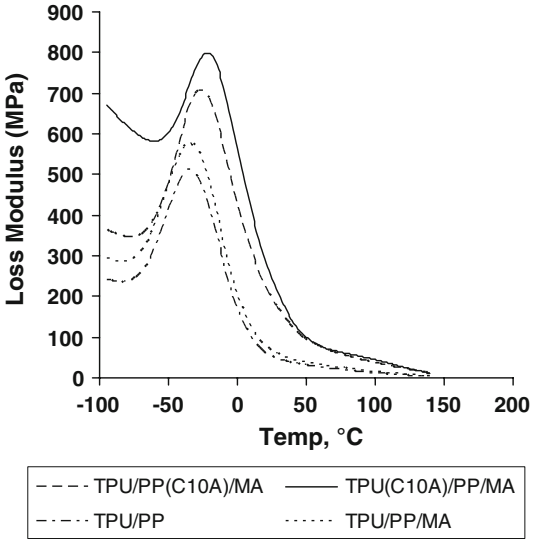

Fig. 5 DMA analysis: E'' versus temperature (10 Hz)

Table 3 Storage modulus (E')

Blend	Storage modulus, E′ (MPa)				
	−50 °C	0 °C	10 °C	20 °C	30 °C
TPU/PP	4950	408	215	151	136
TPU/PP/MA-g-PP	8120	2555	2039	1679	1386
TPU/PP(C10A)/MA-g-PP	10071	3613	2812	2250	1822
TPU(C10A)/PP/MA-g-PP	10956	4255	3291	2638	2099

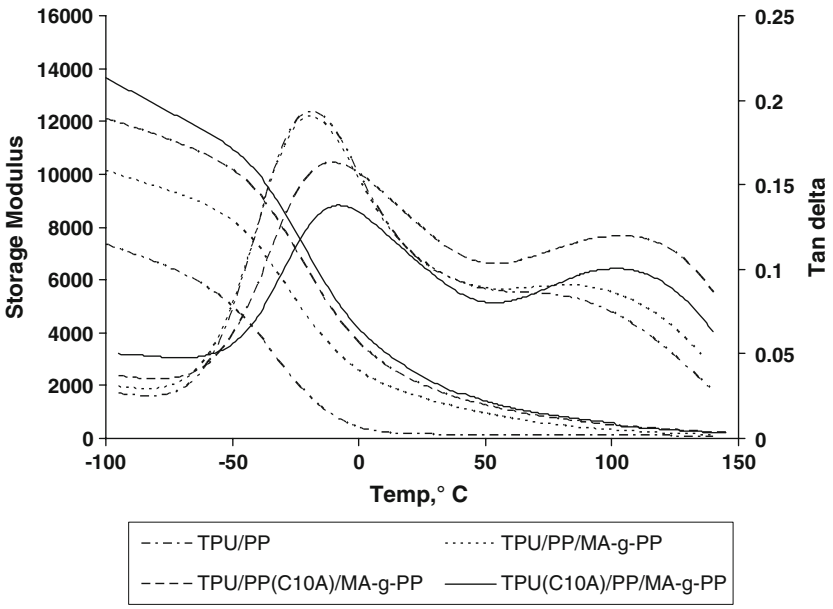

Fig. 4 DMA analysis: E' and tan δ versus temperature (10 Hz)

Table 4 T_g from E'' and tan δ

Material	T_g (°C) from E″	T_g (°C) from Tan δ
TPU/PP	−33.6	−18.5
TPU/PP/MA-g-PP	−32.0	−17.0
TPU/PP(C10A)/MA-g-PP	−25.0	−10.0
TPU(C10A)/PP/MA-g-PP	−19.0	−8.0

same order. DMA and DSC experiments are based on different concepts and hence the numerical values may not match.

In the case of sequence I, the effect of nanoclay is fully utilized by changing the surface tension of the TPU hard segment from around 45 dynes/cm to around 30 dynes/cm [12]. This change in surface tension favours for better dispersion of PP in TPU material, and also the hydroxyl group of the silicate layers forms hydrogen bonds with the carbonyl groups of TPU and maleic anhydride moieties. In the case of sequence II, the dispersion and the reaction of nanoclay with TPU was reduced since nanoclay is first added to PP.

Tensile test

The tensile test data of the nanocomposites and blends are summarized in Table 5. Stress values at 20, 100 and 200% elongations are shown in Fig. 6. The tensile tests indicate that TPU(C10A)/PP/MA-g-PP materials have better tensile properties than TPU/PP(C10A)/MA-g-PP materials. In these materials, when the elongation exceeded 800–900% slippage of specimen from grips was observed; hence elongation at break is not reported. Stress at 20, 100 and 200% elongations increased as a result of blending with PP. Compatibilized TPU blend nanocomposites exhibited higher stresses at the respective elongations than the uncompatibilized blends [18]. The tensile test results substantiated the effect offered by nanoclay as seen earlier in the DMA results.

Fourier transform infra-red spectroscopy

Figure 7a–d shows the FTIR spectra of TPU/PP, TPU/PP/MA-g-PP, TPU/PP(C10A)/MA-g-PP and TPU(C10A)/PP/MA-g-PP blend systems, respectively. Three significant peaks are considered for discussion. Peak at 3340 cm^{-1} wave number represents the hydrogen bonded –NH group. Peak at 1730 cm^{-1} and peak at 1700 cm^{-1} wave number represents free –C=O (carbonyl) and hydrogen bonded –C=O, respectively.

Table 5 Tensile properties of ester–TPU based blends

Blend	Stress at % elongation (MPa)		
	20%	100%	200%
TPU/PP	3.50	4.10	4.30
TPU/PP/MA-g-PP	5.32	5.75	6.10
TPU/PP(C10A)/MA-g-PP	5.90	6.60	6.70
TPU(C10A)/PP/MA-g-PP	7.60	10.10	10.40

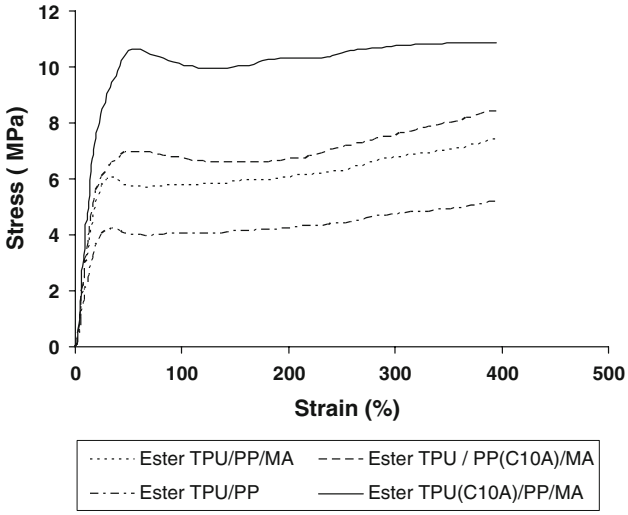

Fig. 6 Tensile test: stress–strain curve

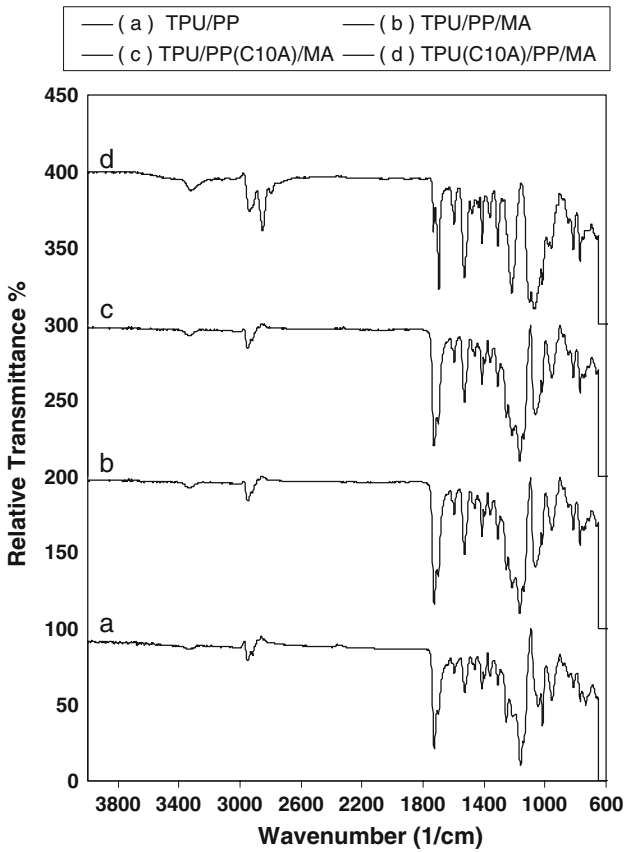

Fig. 7 FTIR analysis

The –NH groups in the urethane linkage of TPU/PP composition form hydrogen bonds [20] with carbonyls of other urethanes in TPU hard segments and with carbonyl group in the soft segments of TPU. In the case of TPU/PP/MA-g-PP composition –NH groups form additional hydrogen bonding with maleic anhydride group of compatibiliser. In the case of TPU(C10A)/PP/MA-g-PP and TPU/PP(C10A)/MA-g-PP composition –NH groups form further hydrogen bonding with oxygen group of silicate layers of nanoclay. The increase of hydrogen bonding is reflected in the FTIR spectra by increase of 3340 cm^{-1} peak intensity. The peak intensity of hydrogen bonded –NH group increases in the order: TPU/PP < TPU/PP/MA-g-PP < TPU/PP(C10A)/MA-g-PP < TPU(C10A)/PP/MA. The intensity of 1730 cm^{-1} peak decreases and intensity of 1700 cm^{-1} peak increases from a to d of Fig. 8. The –C=O of ester–TPU hard and soft segments form hydrogen bonds with –NH group of urethane linkage leading to free –C=O peak and hydrogen bonded –C=O peak corresponding to 1730 cm^{-1} peak and 1700 cm^{-1} of Fig. 8a. In the case of Fig. 8b, –C=O forms additional hydrogen bonding with maleic anhydride group and in Fig. 8c, d, –C=O forms further hydrogen bonding with hydroxyl groups of nanoclay silicate layer. Hence, the intensity of 1730 cm^{-1} peak decreases and intensity of 1700 cm^{-1} peak increases from Fig. 8a to d.

SEM analysis

SEM micrographs of chemically etched (PP material was removed by xylene at 105 °C) surfaces of the TPU/PP, TPU/PP/MA-g-PP, TPU/PP(C10A)/MA-g-PP and TPU(C10A)/PP/MA-g-PP are shown in Fig. 8. It is observed that the size of dispersed PP particle is considerably reduced in TPU(C10A)/PP/MA-g-PP. For nanocomposite SEM sample preparation, the PP portion was removed by chemical etching method which gives very fine holes. In non-clay polymer blends also PP was removed by etching; however, the PP domains are not as fine as clay nanocomposites due to high interfacial tension between TPU and PP and hence fine holes are not evident in SEM micrographs.

As mentioned in the introductory chapter, the high polarity difference between thermoplastic polyurethane and polypropylene limits the miscibility of their blends. Nanoclay was used to reduce the surface energy of the TPU hard segments and makes them more compatible with the non-polar PP. More miscible blends have been obtained by using MA-g-PP as the compatibilizer. Better dispersion of organoclay may be attributed to two reasons. First, maleic anhydride forms hydrogen bonds with the hydroxyl groups of the silicate layers. Second, there is a possible chemical reaction between maleic anhydride and the urethane

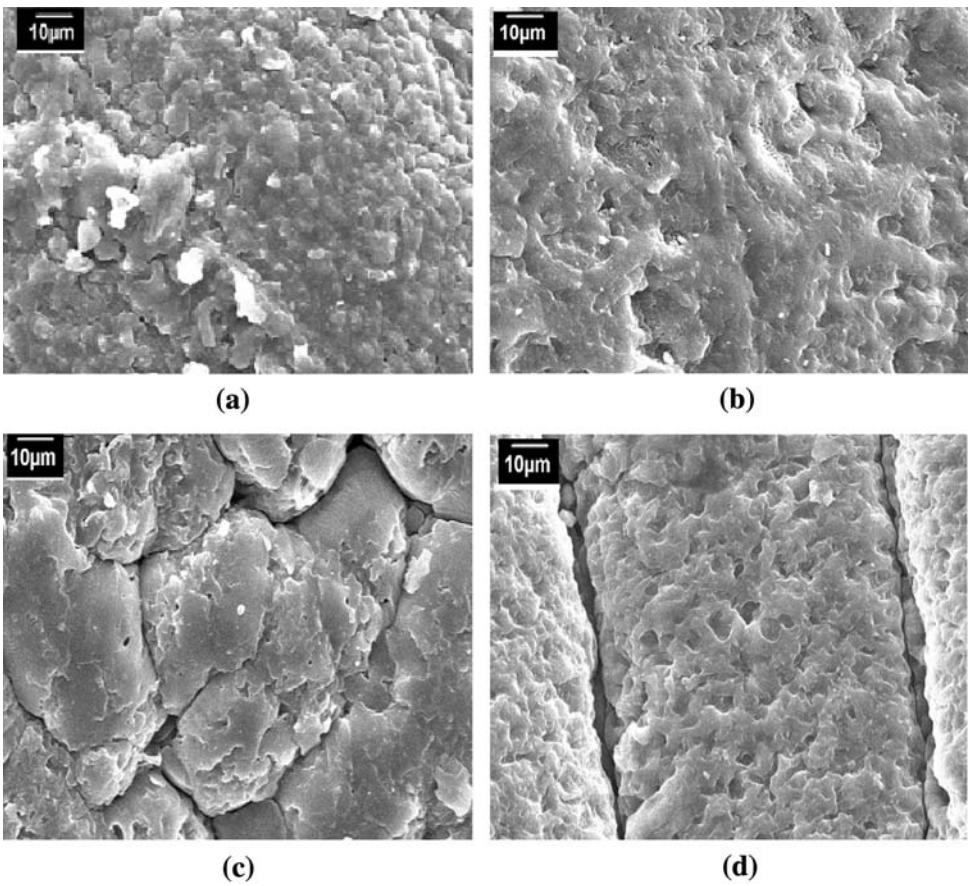

Fig. 8 SEM micrograph. **a** TPU/PP, **b** TPU/PP/MA, **c** TPU/PP(C10A)/MA, and **d** TPU(C10A)/PP/MA

linkages in the TPU hard segments. Compared to the sequence II blend nanocomposites, the sequence I blends show better miscibility as confirmed by XRD, DMA, tensile strength, DSC and SEM analysis. The clear difference between sequence I and sequence II is that the case of sequence I the effect of nanoclay is fully utilized by changing the surface tension of the TPU hard segment from around 45 dynes/cm to around 30 dynes/cm. This change in surface tension favours for better dispersion of PP in TPU material, and also hydroxyl group of silicate layers forms hydrogen bonding with the carbonyl group of TPU and maleic anhydride moieties.

Conclusion

In the present work, studies were made on nanoclay filled MA-g-PP compatibilized TPU/PP blends by considering the sequence of nanoclay addition. These blends were characterized by DMA, DSC, tensile test, FTIR, XRD and SEM analysis. Compared to sequence II blend nanocomposites, the sequence I shows better miscibility. The clear difference between sequence I and sequence II is that the effect of nanoclay is fully utilized for changing the surface tension of TPU hard segment in sequence I. The hydroxyl group of silicate layers form hydrogen bonding with the carbonyl group of TPU and maleic anhydride moieties leading to reduction in surface tension of TPU hard segment from 45 dynes/cm to 30 dynes/cm. This change in surface tension favours for better dispersion of PP in TPU material.

References

1. Holden G, Legge NR, Quirk R, Schroder HE (1996) Thermoplastic elastomers, vol 2. Hanser, Munich
2. Lamba MK, Woodhouse KA, Cooper SL (1988) Polyurethane in biomedical applications. CRC Press, New York
3. Szycher M (1999) Szycher's handbook of polyurethanes. CRC Press, New York
4. Berta M, Lindsay C, Pans G, Camino G (2006) Polym Degrad Stabil 91:1179
5. Jiawen X, Yunhang L, Xiaohui Y, Xinling W (2004) Polym Degrad Stabil 86:549
6. Potschke P, Wallheinke K, Fritsche H, Stutz H (1997) J Appl Polym Sci 64:749
7. Wallheinke K, Potschke P, Stutz HJ (1997) J Appl Polym Sci 65:2217
8. Potschke P, Wallheinke K (1999) Polym Eng Sci 39(6):1035
9. Wallheinke K, Potschke P (1999) Polym Eng Sci 39(6):1022–1034
10. Potschke P, Pionteck J, Stutz H (2002) Polymer 43:6965
11. Lu QW, Macosko CW, Horrion J (2003) Macromol Symp 198:221
12. Lu QW, Macosko CW (2004) Polymer 45:1981
13. Lu QW, Hoye TR, Macosko CW (2002) J Polym Sci A Polym Chem 40:2310
14. Song M, Xia HS, Yao KJ, Hourston DJ (2005) Eur Polym J 41:259
15. Strankowski M, Haponiuk JT, Gazda M, Janik H (2005) e-polymers p_023:1
16. Lertwimolnun W, Vergnes B (2005) Polymer 46:3462
17. Finnigan B, Martin D, Halley P, Truss R, Cambell K (2004) Polymer 45:2249
18. Dan CH, Lee MH, Kim YD, Min BH, Kim J (2006) Polymer 47:6718
19. Chen-chi MM, Hsun-yu S, Hsu-Chiang K, Chen-feng K, Chin-Lung C (2005) J Polym Sci B Polym Phys 43:1076
20. Chun BC, Cho TK, Chong MH, Chung YC, Chen J, Martin D (2007) J Appl Polym Sci 106:712
21. Chang J, Yeong UA (2002) J Polym Sci B Polym Phys 40:670
22. Chavarria F, Paul DR (2006) Polymer 47:7760
23. Pattanayak A, Jana SC (2005) Polymer 46:3228
24. Pattanayak A, Jana SC (2005) Polymer 46:3394
25. Giulina G, Mariarosaria T, Vittoria V (2005) J Polym Sci B Polym Phys 43:2454
26. Pattanayak A, Jana SC (2005) Polymer 46:5183
27. Yao KJ, Song M, Hourston DJ, Luo DZ (2002) Polymer 43:1017
28. Tortora M, Gorrasi G, Vittoria V, Galli G (2002) Polymer 43:6147
29. Kim BK, Seo JW, Jeong HM (2003) Eur Polym J 39:85